


Chaos and Quantum Scars in Bose-Josephson Junction Coupled to a Bosonic Mode

Sudip Sinha and S. Sinha *Indian Institute of Science Education and Research-Kolkata, Mohanpur, Nadia 741246, India*

(Received 7 January 2020; accepted 31 August 2020; published 23 September 2020)

We consider a model describing Bose-Josephson junction (BJJ) coupled to a single bosonic mode exhibiting quantum phase transition (QPT). Onset of chaos above QPT is observed from semiclassical dynamics as well from spectral statistics. Based on entanglement entropy, we analyze the ergodic behavior of eigenstates with increasing energy density which also reveals the influence of dynamical steady state known as π -mode on it. We identify the imprint of unstable π -oscillation as many body quantum scar (MBQS), which leads to the deviation from ergodicity and quantify the degree of scarring. Persistence of phase coherence in nonequilibrium dynamics of such initial state corresponding to the π -mode is an observable signature of MBQS which has relevance in experiments on BJJ.

DOI: 10.1103/PhysRevLett.125.134101

Introduction.—Ergodicity in closed quantum system has attracted attention in recent years due to its implication in variety of interesting phenomena related to the nonequilibrium dynamics of quantum many body system [1,2]. The emergence of steady states in nonequilibrium dynamics of certain many body systems and its correspondence to the generalized Gibbs ensemble is an evidence of thermalization [3–8]. The eigenstate thermalization hypothesis (ETH) has been proposed to explain thermalization of such closed quantum systems at the level of individual eigenstates, [9–11] and its connection with random matrix theory (RMT) has thoroughly been explored theoretically [12–16]. On the other hand, there are certain many body systems which fail to thermalize and remain localized, giving rise to many body localization (MBL) [17–20] phenomena [21–27]. Both the extreme phenomena are related to the degree of ergodicity of closed quantum system, which is a subject of intense study. As an alternate route to thermalization and delocalization, underlying chaotic behavior has also been investigated in certain many body systems [28,29]. Because of easy tunability of parameters, the ultracold atomic system has become a test bed to study both the MBL and nonequilibrium many body dynamics related to ergodicity [22,30–37].

Nonergodic multifractal wave functions are intermediate between localized and extended states, which have been observed in disordered as well as other many body systems [38–42], giving rise to nonergodic behavior such as anomalous thermalization, nonergodic to ergodic transition, and deserves further investigation [43–48].

Apart from above mentioned phenomena, there are other means by which a quantum system can deviate from ergodicity and certain states may lead to the breakdown of ETH hypothesis. In a recent experiment on chain of ultracold Rydberg atoms [49], the appearance of revival

phenomena for certain specific initial states indicating the deviation from ergodicity has been attributed to the existence of many body quantum scars (MBQS) and its underlying mechanism has been analyzed theoretically in a series of recent works [50–54]. After this experiment, MBQS has also been identified theoretically in other models [55,56] as well in a recent experiment on dipolar gas [57]. Quantum scar in single particle wave function can be identified as reminiscence of unstable classical periodic orbits, which was first studied in the context of chaotic stadium [58]. However, in quantum many body system, the correspondence between scarred state and unstable classical orbits is not very obvious. Similarly, the connection between ergodicity in interacting quantum system and underlying chaotic dynamics remains unclear and deserves further investigation. Identifying such scar as reminiscence of unstable collective mode of many body system and to detect its imprint on ergodicity are main focus of the present study.

In this work, we investigate the effect of dynamical steady states on ergodic behavior and formation of quantum scars in a BJJ coupled to a single bosonic mode, which exhibits quantum phase transition (QPT) accompanied by onset of chaos. Similar connection between quantum scar in an interacting system and unstable dynamical modes of its classical counterpart can also be explored in collective spin models [59]. We quantify the ergodic behavior of the states from entanglement entropy (EE), which is summarized in Fig. 1. Interestingly, the presence of a dynamical steady state known as π -oscillation of BJJ [60–62] at an energy density E_0 gives rise to deviation from ergodicity and its imprint remains as scar in the wave function. Within single mode approximation, BJJ with fixed number of bosons N can be described as two site Bose-Hubbard model [63], $\hat{\mathcal{H}}_{\text{BJJ}} = -(J/2)(\hat{a}_L^\dagger \hat{a}_R + \hat{a}_R^\dagger \hat{a}_L) + (U/2N)[\hat{n}_L(\hat{n}_L - 1) + \hat{n}_R(\hat{n}_R - 1)]$, where J and U represent

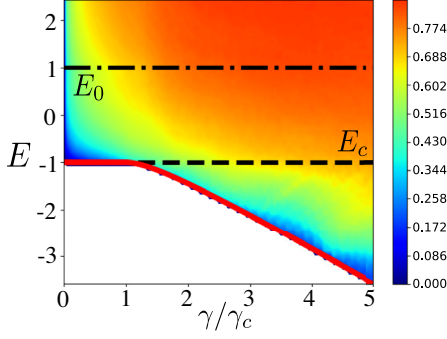


FIG. 1. Ergodic behavior of BJJ based on relative entanglement entropy $S_{\text{en}}/S_{\text{max}}$ (in color scale) of eigenstates with energy density E across the QPT ($\gamma/\gamma_c = 1$). Different FPs: ground state (red solid line), unstable FP-II at E_c (dashed line), and FP-III corresponding to π -mode at E_0 (dashed-dotted line). Parameters chosen: $S = 30$, $\omega_0 = 3$ and for all figures $U = 0.5$, $N_{\text{max}} = 99$.

the hopping strength and on-site interaction, respectively, while $\hat{a}_{L/R}$ and $\hat{n}_{L/R}$ denote annihilation and number operators of boson in respective sites. The steady states and dynamics of BJJ have been studied extensively both experimentally [61,64,65] and theoretically [60–63,66–77].

Model.—Using the Schwinger boson representation $\hat{S}_x = (\hat{a}_R^\dagger \hat{a}_L + \hat{a}_L^\dagger \hat{a}_R)/2$ and $\hat{S}_z = (\hat{n}_R - \hat{n}_L)/2$, $\hat{\mathcal{H}}_{\text{BJJ}}$ represents a large spin system with magnitude $S = N/2$; as a result, the BJJ coupled to a single bosonic mode can be described by the following spin Hamiltonian [77]:

$$\hat{\mathcal{H}} = -J\hat{S}_x + \frac{U}{2S}\hat{S}_z^2 + \frac{\lambda\hat{S}_z}{2\sqrt{2}S}(\hat{b} + \hat{b}^\dagger) + \hbar\omega_0\hat{b}^\dagger\hat{b}, \quad (1)$$

where λ is the coupling strength and \hat{b} is annihilation operator of the bosonic mode with energy $\hbar\omega_0$. We redefine effective coupling strength as $\gamma = \lambda^2/\omega_0$ and scale energy (time) in units of J ($1/J$) with $\hbar = 1$.

Semiclassical analysis.—For $S = N/2 \gg 1$, the spin system is treated semiclassically by the wave function $|\Psi_{\text{sc}}\rangle = |z, \phi\rangle \otimes |\alpha\rangle$, where $|z, \phi\rangle$ and $|\alpha\rangle$ represent the coherent states of the spin and boson, respectively [78]. The variables ϕ and $z = \cos\theta$ are canonical conjugate coordinates describing the orientation of the classical spin vector $\vec{S} = (S \sin\theta \cos\phi, S \sin\theta \sin\phi, S \cos\theta)$ while $\alpha = \sqrt{2S}(q + ip)/2$ denotes the dimensionless coordinates of the corresponding oscillator. In BJJ, z and ϕ denote the number imbalance (magnetization) and relative phase between the two sites, respectively [63]. The corresponding classical Hamiltonian is given by [77]

$$\mathcal{H}_{\text{cl}} = -\sqrt{1-z^2}\cos\phi + \frac{U}{2}z^2 + \frac{\lambda}{2}zq + \frac{\omega_0}{2}(q^2 + p^2). \quad (2)$$

The classical energy E and \mathcal{H}_{cl} are scaled by S to make them intensive. In isolated BJJ with $U > 0$, the interaction is antiferromagnetic and the spin vector is aligned along the

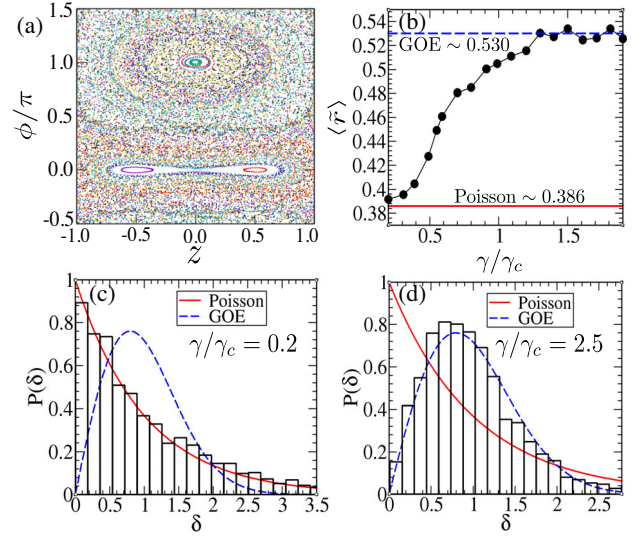


FIG. 2. Onset of chaos: (a) classical phase portrait for $\gamma/\gamma_c = 1.11$, $\omega_0 = 3.0$, and $U = 0.5$. (b) Crossover of $\langle \tilde{r} \rangle$ from Poisson (red solid line) to GOE values (blue dashed line) by tuning γ . (c),(d) Level spacing distributions for $\gamma < \gamma_c$ and $\gamma > \gamma_c$, respectively. Parameters chosen: $S = 25$ and for (b)–(d) $\omega_0 = 1.0$. For spectral statistics, first 1400 energy levels are considered from the even parity sector [80].

x -axis giving $z = 0$. Whereas in the presence of bosonic mode, the effective interaction $\tilde{U} = U - \gamma/4$ can become ferromagnetic, due to which BJJ undergoes a QPT at $\gamma_c = 4(1 + U)$ to a state having finite imbalance ($z \neq 0$) [77]. Such transition has also been confirmed from full quantum analysis [79]. The equation of motion (EOM) for collective coordinates can be obtained from Hamilton's equations [77,79]

$$\dot{\vec{X}} = \frac{\partial \mathcal{H}_{\text{cl}}}{\partial \vec{P}}, \quad \dot{\vec{P}} = -\frac{\partial \mathcal{H}_{\text{cl}}}{\partial \vec{X}}, \quad (3)$$

where $\vec{X} = \{\phi, q\}$ and $\vec{P} = \{z, p\}$ are canonical conjugates of each other. The fixed points (FPs) obtained from the EOM and their stability are analyzed near QPT [77]. For $\gamma > \gamma_c$, we categorize the FPs as I. symmetry broken: $\{z = \pm\sqrt{1 - (1/\tilde{U})^2}, \phi = 0, q = \mp\sqrt{\gamma z^2/4\omega_0}, p = 0\}$ with energy density $E_{\text{GS}} = -\frac{1}{2}(1/|\tilde{U}| + |\tilde{U}|)$, II. symmetry unbroken: $\{z = 0, \phi = 0, q = 0, p = 0\}$ with energy density $E_c = -1$, and III. corresponds to π -oscillation: $\{z = 0, \phi = \pi, q = 0, p = 0\}$ [60,77] with energy density $E_0 = 1$. The stable FPs corresponding to I and III are visible in classical phase portrait [Fig. 2(a)]. Influence of this π -mode on ergodic behavior of the system is the main focus of the present study.

Ergodicity and chaos.—Phase space trajectories corresponding to semiclassical dynamics of BJJ can be studied from Eq. (3) [77]. In Fig. 2(a), the phase portrait reveals chaotic dynamics near QPT indicating ergodic behavior. To

analyze the system quantum mechanically, we obtain eigenvalues \mathcal{E}_n and eigenfunctions $|\psi_n\rangle = \sum_i^N \psi_n^i |i\rangle$ of the Hamiltonian [Eq. (1)] using the basis states $|i\rangle = |m_z, n\rangle$, where m_z and n are eigenvalues of \hat{S}_z and number operator for bosonic mode, respectively, where the latter is truncated to N_{\max} for numerical calculation. The dimension of the associated Hilbert space is $\mathcal{N} = (2S + 1)(N_{\max} + 1)$. The eigenvectors and corresponding eigenvalues can be divided into even and odd sector of parity operator $\hat{\Pi} = e^{i\pi\hat{P}}$, where $\hat{P} = \hat{n} - \hat{S}_x + S$. The occurrence of excited state quantum phase transition at FP-II leads to the suppression of energy gap between the consecutive even and odd parity states below E_c separating the symmetry broken and unbroken states [79,81–85]. To investigate the signature of chaos at the quantum level, we study the spectral properties. The eigenvalues \mathcal{E}_n of each parity sector are sorted in ascending order, and spacing distribution $P(\delta)$ of the level spacing $\delta_n = \mathcal{E}_{n+1} - \mathcal{E}_n$ is obtained following the usual prescription [86,87]. According to Bohigas-Giannoni-Schmit conjecture [88], the level spacing distribution of classically chaotic system follows Wigner-Dyson (WD) statistics, whereas Poissonian statistics, $P(\delta) = \exp(-\delta)$ can be observed in regular (integrable) regime [86,89]. For weak coupling strength $\gamma < \gamma_c$, the level spacing follows Poisson distribution as evident from Fig. 2(c). On the other hand, for increasing γ above γ_c , the level spacing distribution resembles WD statistics, $P(\delta) = (\pi\delta/2) \exp(-\pi\delta^2/4)$ corresponding to Gaussian orthogonal ensemble (GOE) of RMT [see Fig. 2(d)]. Onset of chaos is also evident from the average value of level spacing ratio defined as $\langle \tilde{r} \rangle = \langle \min(\delta_n, \delta_{n+1}) / \max(\delta_n, \delta_{n+1}) \rangle$, which shows a crossover from Poissonian limit with $\langle \tilde{r} \rangle \sim 0.386$ to GOE limit with $\langle \tilde{r} \rangle \sim 0.530$ [90] across the QPT as seen in Fig. 2(b). Such spectral analysis indicates chaotic behavior above QPT; however, a detailed study of eigenvectors can reveal more interesting phenomena related to ergodicity and nonequilibrium dynamics.

Effect of steady states on ergodic behavior.—In order to quantify the degree of ergodicity, we study the EE of energy eigenstates, which is also relevant for understanding nonequilibrium properties of the BJJ. By tracing out the bosonic degrees, we obtain the reduced density matrix of the spin sector, $\hat{\rho}_S = \text{Tr}_B |\psi\rangle\langle\psi|$ and corresponding EE, $S_{\text{en}} = -\text{Tr}(\hat{\rho}_S \log \hat{\rho}_S)$. To quantify the ergodic nature of a state, we compare it with the EE of maximally random state partitioned into subsystems $A(B)$ with dimensionality $\mathcal{D}_A(\mathcal{D}_B)$ [91]. Maximum EE corresponding to smaller subsystem A with $\mathcal{D}_A \ll \mathcal{D}_B$ can be written as

$$S_{\text{max}} \simeq \log(\mathcal{D}_A) - O(\mathcal{D}_A/2\mathcal{D}_B). \quad (4)$$

For the present system $\mathcal{D}_A = 2S + 1$, $\mathcal{D}_B = N_{\max} + 1$ represents dimensions of spin and bosonic sector, respectively. Relative EE, $S_{\text{en}}/S_{\text{max}}$ is obtained for eigenstates with increasing energy density E and varying the coupling

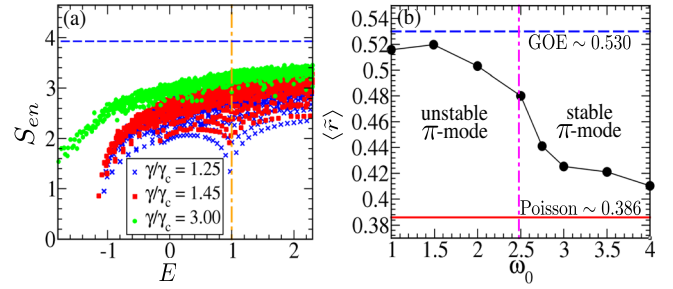


FIG. 3. (a) EE of eigenstates with increasing energy density E for different γ/γ_c for $\omega_0 = 3$. Vertical dashed-dotted line: energy density E_0 of π -oscillation and horizontal dashed line: S_{max} . (b) Variation of $\langle \tilde{r} \rangle$ with ω_0 for fixed $\gamma/\gamma_c = 1.2$. The pink dashed-dotted line at $\omega_0 = 2.48$ divides the region of stability of π -mode. Parameters chosen: $S = 25$.

γ , which is shown as color scale plot in Fig. 1, summarizing the ergodic behavior of the BJJ across QPT. It is evident from Figs. 1 and 3(a), above QPT, the EE of states increases monotonically with energy density E and approaches the maximum limit [given by Eq. (4)], suggesting a crossover from nonergodic to weak ergodic behavior which can also be confirmed from the nonequilibrium dynamics of BJJ [79]. A recent study shows such relative EE of a subsystem below its maximum limit can indicate nonergodic (multifractal) nature of states [92]. Similar behavior in degree of chaos has also been observed in Dicke model [82,93].

Interestingly, in the weakly ergodic regime, the presence of π -mode at an energy density $E_0 = 1$ (FP-III) can influence the ergodic properties. Stable π -oscillation can exist above QPT and becomes dynamically unstable at a coupling strength,

$$\gamma_u = (\omega_0^2 + U - 1)^2 / \omega_0^2. \quad (5)$$

As seen from Fig. 3(a), a dip in EE appears at E_0 due to the presence of such stable π -oscillation which gradually vanishes above γ_u . By increasing the frequency of the bosonic mode ω_0 , enhanced stability of the π -mode and suppression of chaos is observed around the energy density $E = E_0$ [79], which is also reflected from the decrease in $\langle \tilde{r} \rangle$ with ω_0 , as the unstable π -mode becomes stable [see Fig. 3(b)] [94].

Quantum scar of π -oscillation.—To search for imprint of unstable π -mode above the coupling strength γ_u , we closely analyze the eigenstates $|\psi_n\rangle$ within a small window of energy density around E_0 . Unlike EE, Shannon entropy (SE) of states, $S_{\text{Sh}} = -\sum_i |\psi_n^i|^2 \log |\psi_n^i|^2$ within this window reveals an interesting structure as shown in Fig. 4(a). The SE of most of the states forms a bandlike structure below its GOE limit $\log(0.48\mathcal{N})$ [12,15], whereas a few states with lower SE are deviated from this band. We identify scar of unstable π -oscillation in these deviated states, which become evident from the Husimi distribution $Q(z, \phi) = (1/\pi) \langle z, \phi | \hat{\rho}_S | z, \phi \rangle$ of reduced density matrix $\hat{\rho}_S$

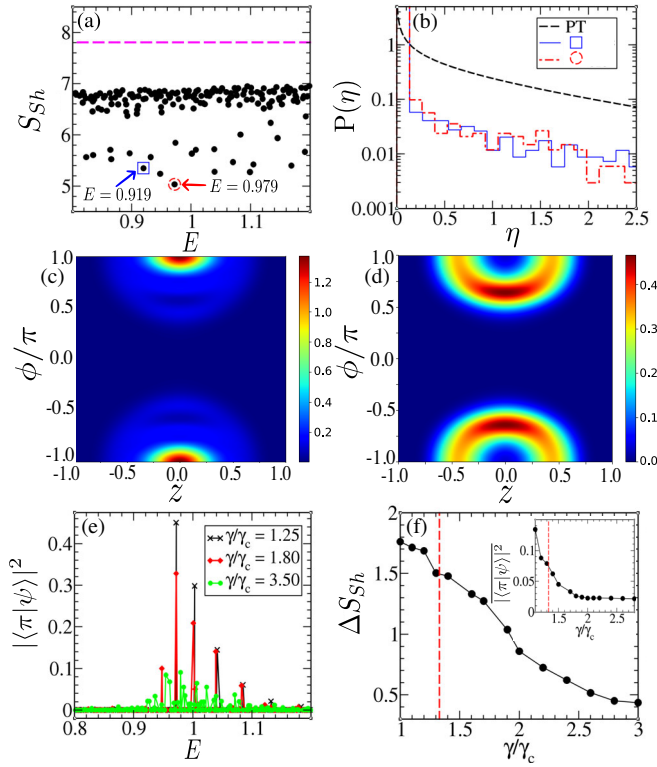


FIG. 4. MBQS of π -mode at E_0 : (a) Shannon entropy in a small window near $E \approx E_0$. Horizontal dashed line represents the GOE limit. (b) Distribution $P(\eta)$ of scarred states [marked in (a)] at $\gamma = 1.8\gamma_c$. Husimi distribution $Q(z, \phi)$ of scarred states marked by (c) red circle and (d) blue square in (a). (e) Overlap of eigenstates with π -mode. Degree of scarring: (f) variation of ΔS_{Sh} ($|\langle \pi | \psi \rangle|^2$ in the inset) with increasing γ/γ_c . Vertical red line denotes instability of π -mode at $\gamma_u = 1.33\gamma_c$. Parameters chosen: $S = 25$ and $\omega_0 = 3.0$.

as depicted in Figs. 4(c) and 4(d). We also find that certain eigenstates around energy density E_0 have large overlap with the coherent state $|\pi\rangle = |z = 0, \phi = \pi\rangle \otimes |q = 0, p = 0\rangle$, describing the steady state FP-III of π -mode. The state with maximum overlap with $|\pi\rangle$ state turns out to be the most deviated state [marked by circle in Fig. 4(a)] due to the scar of π -mode which is visible from its Husimi distribution with maximum phase space density at $\{z = 0, \phi = \pi\}$ [see Fig. 4(c)]. More interestingly, the Husimi distribution of another deviated state [marked by square in Fig. 4(a)] exhibits scar of an orbit around FP-III, corresponding to unstable π -oscillation [see Fig. 4(d)]. The trajectories around steady state of π -mode are also unstable with positive Lyapunov exponent and scar of such unstable π -oscillations is observed below energy density E_0 . Next, we analyze the statistical properties of the wave function of such scarred states and compute the distribution $P(\eta)$ of the scaled elements $\eta = |\psi_n^i|^2 \mathcal{N}$, which significantly deviates from Porter-Thomas distribution $P(\eta) = (1/\sqrt{2\pi\eta}) \exp(-\eta/2)$ [86] of eigenvectors of GOE matrices [see Fig. 4(b)]. This indicates non-Gaussian distribution

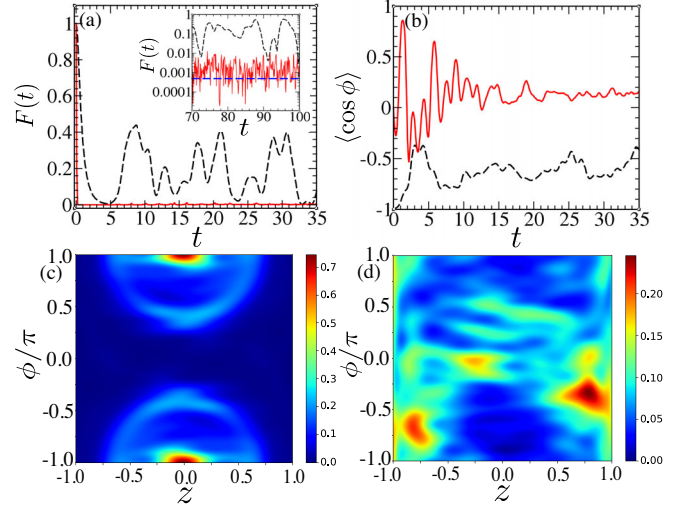


FIG. 5. Time evolution of $|\pi\rangle$ state (black dashed curve) and arbitrary state $|z = 0.60, \phi = \pi/2\rangle \otimes |q = 0.40, p = 0.0\rangle$ (red solid curve) at $E \approx E_0$ shown by (a) survival probability $F(t) = |\langle \psi(t) | \psi(0) \rangle|^2$ and (b) phase coherence. Inset in (a) shows long time behavior of $F(t)$ compared with GOE limit. (c), (d) show Husimi distribution of $|\pi\rangle$ state and arbitrary state, respectively, after sufficient time $t = 25$. Parameters chosen: $S = 30$, $\gamma = 1.8\gamma_c > \gamma_u$, and $\omega_0 = 3.0$.

of elements ψ_n^i of scarred wave functions leading to the violation of Berry's conjecture [95].

Above γ_u , the instability exponent of π -mode increases as $\text{Im}(\omega) \sim \sqrt{\gamma - \gamma_u}$, which reduces the degree of scarring (DOS) resulting in enhancement of ergodicity. We quantify the DOS from the average deviation ΔS_{Sh} of SE of the scarred states from the band of weakly ergodic states. Both ΔS_{Sh} and the average overlap $|\langle \pi | \psi \rangle|^2$ decrease with increasing coupling γ , as shown in Fig. 4(f), indicating reduction of DOS. As a result of enhanced ergodicity, the corresponding distribution $P(\eta)$ also approaches to GOE limit with increasing γ .

Effect of such quantum scar can also be observed from anomalous behavior of nonequilibrium dynamics. Time evolution of the $|\pi\rangle$ state exhibits interesting features compared to any other arbitrary state at similar energy density (see Fig. 5). Survival probability $F(t) = |\langle \psi(t) | \psi(0) \rangle|^2$ of this initial state shows oscillatory behavior and in long time deviates significantly from the GOE limit $3/\mathcal{N}$ [14,15] compared to other initial states [see Fig. 5(a)]. Also, the Husimi distribution of the final state in the time evolution retains the scar of $|\pi\rangle$ state [see Fig. 5(c)]. From the phase operator $\hat{\phi}$ [79,96] defining the relative phase between two sites of BJJ, we calculate $\langle \cos \phi \rangle$ quantifying the phase coherence [96–98]. Remarkably, such phase coherence persists during the time evolution of $|\pi\rangle$ state in contrast to its decay in ergodic dynamics [see Fig. 5(b)], which can serve as an experimentally observable effect of quantum scar.

Conclusion.—BJJ coupled to a single bosonic mode constitutes an interesting model exhibiting QPT, onset of chaos, and athermal behavior related to quantum scars. We identify quantum scars related to collective π -oscillation and quantify degree of scarring. In contrast to ergodic dynamics, phase coherence is retained during time evolution for special choice of initial state corresponding to π -mode, which is a detectable signature of MBQS relevant for experiments on BJJ [98]. This model can also be realized in experiment by coupling a BJJ with cavity mode similar to the experiments in [99,100] and also in circuit QED setup [101]. In the absence of interaction ($U = 0$), the present model reduces to Dicke model [102], which is also a promising candidate to study the effect of quantum scarring, due to its experimental realization [99,100].

The present study elucidates the formation of scar in an interacting quantum system and its connection with underlying collective dynamics, which can also be explored in other systems [59].

We thank Hans Kroha for discussion.

-
- [1] A. Polkovnikov, K. Sengupta, A. Silva, and M. Vengalattore, *Rev. Mod. Phys.* **83**, 863 (2011).
- [2] E. Altman, [arXiv:1512.00870](https://arxiv.org/abs/1512.00870).
- [3] M. Rigol, V. Dunjko, V. Yurovsky, and M. Olshanii, *Phys. Rev. Lett.* **98**, 050405 (2007); M. Rigol, V. Dunjko, and M. Olshanii, *Nature (London)* **452**, 854 (2008).
- [4] T. Langen, S. Erne, R. Geiger, B. Rauer, T. Schweigler, M. Kuhnert, W. Rohringer, I. E. Mazets, T. Gasenzer, and J. Schmiedmayer, *Science* **348**, 207 (2015).
- [5] M. Gring, M. Kuhnert, T. Langen, T. Kitagawa, B. Rauer, M. Schreitl, I. Mazets, D. A. Smith, E. Demler, and J. Schmiedmayer, *Science* **337**, 1318 (2012).
- [6] J.-S. Caux and R. M. Konik, *Phys. Rev. Lett.* **109**, 175301 (2012).
- [7] S. Maity, U. Bhattacharya, A. Dutta, and D. Sen, *Phys. Rev. B* **99**, 020306(R) (2019).
- [8] E. Canovi, D. Rossini, R. Fazio, G. E. Santoro, and A. Silva, *Phys. Rev. B* **83**, 094431 (2011).
- [9] J. M. Deutsch, *Phys. Rev. A* **43**, 2046 (1991).
- [10] M. Srednicki, *Phys. Rev. E* **50**, 888 (1994); M. Srednicki, *J. Phys. A* **32**, 1163 (1999).
- [11] P. Reimann, *Phys. Rev. Lett.* **115**, 010403 (2015); **120**, 230601 (2018).
- [12] F. M. Izrailev, *Phys. Rep.* **196**, 299 (1990).
- [13] L. F. Santos and M. Rigol, *Phys. Rev. E* **82**, 031130 (2010).
- [14] E. J. Torres-Herrera, M. Vyas, and L. F. Santos, *New J. Phys.* **16**, 063010 (2014).
- [15] F. Borgonovi, F. M. Izrailev, L. F. Santos, and V. G. Zelevinsky, *Phys. Rep.* **626**, 1 (2016).
- [16] L. D'Alessio, Y. Kafri, A. Polkovnikov, and M. Rigol, *Adv. Phys.* **65**, 239 (2016).
- [17] A. Pal and D. A. Huse, *Phys. Rev. B* **82**, 174411 (2010); R. Nandkishore and D. A. Huse, *Annu. Rev. Condens. Matter Phys.* **6**, 15 (2015); D. A. Abanin and Z. Papić, *Ann. Phys. (Berlin)* **529**, 1700169 (2017); E. Altman, *Nat. Phys.* **14**, 979 (2018).
- [18] R. Nandkishore, S. Gopalakrishnan, and D. A. Huse, *Phys. Rev. B* **90**, 064203 (2014).
- [19] I. L. Aleiner, B. L. Altshuler, and G. V. Shlyapnikov, *Nat. Phys.* **6**, 900 (2010).
- [20] E. J. Torres-Herrera and L. F. Santos, *Phys. Rev. B* **92**, 014208 (2015).
- [21] P. Bordia, H. Lüschen, U. Schneider, M. Knap, and I. Bloch, *Nat. Phys.* **13**, 460 (2017); P. Bordia, H. Lüschen, S. Scherg, S. Gopalakrishnan, M. Knap, U. Schneider, and I. Bloch, *Phys. Rev. X* **7**, 041047 (2017).
- [22] M. Schreiber, S. S. Hodgman, P. Bordia, H. P. Lüschen, M. H. Fischer, R. Vosk, E. Altman, U. Schneider, and I. Bloch, *Science* **349**, 842 (2015).
- [23] L. D'Alessio and A. Polkovnikov, *Ann. Phys. (Amsterdam)* **333**, 19 (2013).
- [24] M. Serbyn, Z. Papić, and D. A. Abanin, *Phys. Rev. X* **5**, 041047 (2015).
- [25] A. Lazarides, A. Das, and R. Moessner, *Phys. Rev. Lett.* **115**, 030402 (2015); E. Bairey, G. Refael, and N. H. Lindner, *Phys. Rev. B* **96**, 020201(R) (2017).
- [26] V. P. Michal, B. L. Altshuler, and G. V. Shlyapnikov, *Phys. Rev. Lett.* **113**, 045304 (2014).
- [27] S. Ray, A. Ghosh, and S. Sinha, *Phys. Rev. E* **97**, 010101 (R) (2018); S. Ray, B. Mukherjee, S. Sinha, and K. Sengupta, *Phys. Rev. A* **96**, 023607 (2017).
- [28] A. Altland and F. Haake, *Phys. Rev. Lett.* **108**, 073601 (2012); A. Altland and F. Haake, *New J. Phys.* **14**, 073011 (2012).
- [29] S. Ray, A. Ghosh, and S. Sinha, *Phys. Rev. E* **94**, 032103 (2016).
- [30] J.-y. Choi, S. Hild, J. Zeiher, P. Schauss, A. Rubio-Abadal, T. Yefsah, V. Khemani, D. A. Huse, I. Bloch, and C. Gross, *Science* **352**, 1547 (2016); K. X. Wei, C. Ramanathan, and P. Cappellaro, *Phys. Rev. Lett.* **120**, 070501 (2018).
- [31] B. Deissler, M. Zaccanti, G. Roati, C. D'Errico, M. Fattori, M. Modugno, G. Modugno, and M. Inguscio, *Nat. Phys.* **6**, 354 (2010); G. Roati, C. D'Errico, L. Fallani, M. Fattori, C. Fort, M. Zaccanti, G. Modugno, M. Modugno, and M. Inguscio, *Nature (London)* **453**, 895 (2008).
- [32] H. P. Lüschen, P. Bordia, S. Scherg, F. Alet, E. Altman, U. Schneider, and I. Bloch, *Phys. Rev. Lett.* **119**, 260401 (2017).
- [33] E. Lucioni, B. Deissler, L. Tanzi, G. Roati, M. Zaccanti, M. Modugno, M. Larcher, F. Dalfovo, M. Inguscio, and G. Modugno, *Phys. Rev. Lett.* **106**, 230403 (2011).
- [34] T. Kinoshita, T. Wenger, and S. D. Weiss, *Nature (London)* **440**, 900 (2006); Y. Tang, W. Kao, K.-Y. Li, S. Seo, K. Mallayya, M. Rigol, S. Gopalakrishnan, and B. L. Lev, *Phys. Rev. X* **8**, 021030 (2018).
- [35] M. A. Garcia-March, S. V. Frank, M. Bonneau, J. Schmiedmayer, M. Lewenstein, and L. F. Santos, *New J. Phys.* **20**, 113039 (2018).
- [36] T. Langen, R. Geiger, and J. Schmiedmayer, *Annu. Rev. Condens. Matter Phys.* **6**, 201 (2015).
- [37] F. Meinert, M. J. Mark, E. Kirilov, K. Lauber, P. Weinmann, A. J. Daley, and H. C. Nagerl, *Phys. Rev. Lett.* **111**, 053003 (2013); J. Eisert, M. Friesdorf, and C. Gogolin, *Nat. Phys.* **11**, 124 (2015).

- [38] M. Janssen, *Phys. Rep.* **295**, 1 (1998); F. Evers and A. D. Mirlin, *Rev. Mod. Phys.* **80**, 1355 (2008); B. L. Altshuler, V. E. Kravtsov, and I. V. Lerner, *JETP Lett.* **43**, 441 (1986).
- [39] J.-M. Stéphan, G. Misguich, and V. Pasquier, *Phys. Rev. B* **84**, 195128 (2011).
- [40] Y. Y. Atas and E. Bogomolny, *Phys. Rev. E* **86**, 021104 (2012); Y. Y. Atas and E. Bogomolny, *Phil. Trans. R. Soc. A* **372**, 20120520 (2014).
- [41] E. J. Torres-Herrera and L. F. Santos, *Ann. Phys. (Berlin)* **529**, 1600284 (2017).
- [42] A. Bäcker, M. Haque, and I. M. Khaymovich, *Phys. Rev. E* **100**, 032117 (2019).
- [43] B. L. Altshuler, E. Cuevas, L. B. Ioffe, and V. E. Kravtsov, *Phys. Rev. Lett.* **117**, 156601 (2016); M. Pino, L. B. Ioffe, and B. L. Altshuler, *Proc. Natl. Acad. Sci. U.S.A.* **113**, 536 (2016); A. De Luca, B. L. Altshuler, V. E. Kravtsov, and A. Scardicchio, *Phys. Rev. Lett.* **113**, 046806 (2014).
- [44] M. Serbyn, Z. Papić, and D. A. Abanin, *Phys. Rev. B* **96**, 104201 (2017); C. Monthus, *J. Stat. Mech.* (2016) 073301.
- [45] X. Deng, S. Ray, S. Sinha, G. V. Shlyapnikov, and L. Santos, *Phys. Rev. Lett.* **123**, 025301 (2019).
- [46] D. J. Luitz and Y. Bar Lev, *Phys. Rev. Lett.* **117**, 170404 (2016); A. Relaño, *Phys. Rev. Lett.* **121**, 030602 (2018).
- [47] T. Micklitz, F. Monteiro, and A. Altland, *Phys. Rev. Lett.* **123**, 125701 (2019).
- [48] W. Buijsman, V. Gritsev, and R. Sprik, *Phys. Rev. Lett.* **118**, 080601 (2017).
- [49] H. Bernien, S. Schwartz, A. Keesling *et al.*, *Nature (London)* **551**, 579 (2017).
- [50] C. J. Turner, A. A. Michailidis, D. A. Abanin, M. Serbyn, and Z. Papić, *Nat. Phys.* **14**, 745 (2018); *Phys. Rev. B* **98**, 155134 (2018).
- [51] C. J. Lin and O. I. Motrunich, *Phys. Rev. Lett.* **122**, 173401 (2019).
- [52] V. Khemani, C. R. Laumann, and A. Chandran, *Phys. Rev. B* **99**, 161101(R) (2019).
- [53] S. Choi, C. J. Turner, H. Pichler, W. W. Ho, A. A. Michailidis, Z. Papić, M. Serbyn, M. D. Lukin, and D. A. Abanin, *Phys. Rev. Lett.* **122**, 220603 (2019).
- [54] T. Iadecola, M. Schecter, and S. Xu, *Phys. Rev. B* **100**, 184312 (2019).
- [55] S. Moudgalya, N. Regnault, and B. A. Bernevig, *Phys. Rev. B* **98**, 235156 (2018); N. Shiraishi, *J. Stat. Mech.* (2019) 083103.
- [56] M. Schecter and T. Iadecola, *Phys. Rev. Lett.* **123**, 147201 (2019).
- [57] W. Kao, K.-Y. Li, K.-Y. Lin, S. Gopalakrishnan, and B. L. Lev, *arXiv:2002.10475*.
- [58] E. J. Heller, *Phys. Rev. Lett.* **53**, 1515 (1984).
- [59] D. Mondal, S. Sinha, and S. Sinha, *Phys. Rev. E* **102**, 020101 (2020).
- [60] A. Smerzi, S. Fantoni, S. Giovanazzi, and S. R. Shenoy, *Phys. Rev. Lett.* **79**, 4950 (1997); S. Raghavan, A. Smerzi, S. Fantoni, and S. R. Shenoy, *Phys. Rev. A* **59**, 620 (1999).
- [61] T. Zibold, E. Nicklas, C. Gross, and M. K. Oberthaler, *Phys. Rev. Lett.* **105**, 204101 (2010).
- [62] A. Pizzi, F. Dolcini, and K. Le Hur, *Phys. Rev. B* **99**, 094301 (2019).
- [63] G. J. Milburn, J. Corney, E. M. Wright, and D. F. Walls, *Phys. Rev. A* **55**, 4318 (1997).
- [64] S. Levy, E. Lahoud, I. Shomroni, and J. Steinmayer, *Nature (London)* **449**, 579 (2007); T. Schumm, S. Hofferberth, L. M. Andersson, S. Wildermuth, S. Groth, I. Bar-Joseph, J. Schmiedmayer, and P. Krger, *Nat. Phys.* **1**, 57 (2005).
- [65] M. Albiez, R. Gati, J. Fölling, S. Hunsmann, M. Cristiani, and M. K. Oberthaler, *Phys. Rev. Lett.* **95**, 010402 (2005).
- [66] B. Juliá-Díaz, D. Dagnino, M. Lewenstein, J. Martorell, and A. Polls, *Phys. Rev. A* **81**, 023615 (2010).
- [67] A. Vardi and J. R. Anglin, *Phys. Rev. Lett.* **86**, 568 (2001).
- [68] D. R. Dounas-Frazer, A. M. Hermundstad, and L. D. Carr, *Phys. Rev. Lett.* **99**, 200402 (2007).
- [69] J. Gillet, M. A. Garcia-March, T. Busch, and F. Sols, *Phys. Rev. A* **89**, 023614 (2014).
- [70] G. Ferrini, A. Minguzzi, and F. W. J. Hekking, *Phys. Rev. A* **78**, 023606 (2008); V. S. Shchesnovich and M. Trippenbach, *Phys. Rev. A* **78**, 023611 (2008).
- [71] I. Zapata, F. Sols, and A. J. Leggett, *Phys. Rev. A* **57**, R28 (1998); **67**, 021603(R) (2003).
- [72] E. Boukobza, M. Chuchem, D. Cohen, and A. Vardi, *Phys. Rev. Lett.* **102**, 180403 (2009); M. Chuchem, K. Smith-Mannschott, M. Hiller, T. Kottos, A. Vardi, and D. Cohen, *Phys. Rev. A* **82**, 053617 (2010); R. J. Kerkdyk and S. Sinha, *J. Phys. B* **46**, 185301 (2013).
- [73] E. Boukobza, M. G. Moore, D. Cohen, and A. Vardi, *Phys. Rev. Lett.* **104**, 240402 (2010).
- [74] M. Trujillo-Martinez, A. Posazhennikova, and J. Kroha, *Phys. Rev. Lett.* **103**, 105302 (2009); M. Trujillo-Martinez, A. Posazhennikova, and J. Kroha, *New J. Phys.* **17**, 013006 (2015).
- [75] D. Witthaut, F. Trimborn, and S. Wimberger, *Phys. Rev. Lett.* **101**, 200402 (2008).
- [76] J. C. Louw, J. N. Kriel, and M. Kastner, *Phys. Rev. A* **100**, 022115 (2019).
- [77] S. Sinha and S. Sinha, *Phys. Rev. E* **100**, 032115 (2019).
- [78] J. M. Radcliffe, *J. Phys. A* **4**, 313 (1971).
- [79] See Supplemental Material at <http://link.aps.org/supplemental/10.1103/PhysRevLett.125.134101> for details of transitions, effect of mode frequency, nonequilibrium dynamics, and scars in the present model.
- [80] For spectral statistics, we have taken energy levels up to a sufficiently high energy density, where the degree of chaos is not changing as well the truncation effect of the Fock space is minimized.
- [81] P. Cejnar, M. Macek, S. Heinze, J. Jolie, and J. Dobeš, *J. Phys. A* **39**, L515 (2006); M. A. Caprio, P. Cejnar, and F. Iachello, *Ann. Phys. (Amsterdam)* **323**, 1106 (2008).
- [82] P. Pérez-Fernández and A. Relaño, J. M. Arias, P. Cejnar, J. Dukelsky, and J. E. García-Ramos, *Phys. Rev. E* **83**, 046208 (2011).
- [83] P. Stránský, M. Macek, and P. Cejnar, *Ann. Phys. (Amsterdam)* **345**, 73 (2014); P. Stránský, M. Macek, A. Leviatan, and P. Cejnar, *Ann. Phys. (Amsterdam)* **356**, 57 (2015).
- [84] T. Brandes, *Phys. Rev. E* **88**, 032133 (2013); P. Pérez-Fernández and A. Relaño, *Phys. Rev. E* **96**, 012121 (2017).
- [85] P. Ribeiro, J. Vidal, and R. Mosseri, *Phys. Rev. E* **78**, 021106 (2008); L. F. Santos, M. Távora, and F. Pérez-Bernal, *Phys. Rev. A* **94**, 012113 (2016).

- [86] F. Haake, *Quantum Signatures of Chaos*, Springer Science and Business Media (Springer, Berlin, Heidelberg, 2013), Vol. 54.
- [87] M. L. Mehta, *Random Matrices*, 3rd ed. (Elsevier, Amsterdam, 2004), Vol. 142.
- [88] O. Bohigas, M. J. Giannoni, and C. Schmit, *Phys. Rev. Lett.* **52**, 1 (1984); *J. Phys. Lett.* **45**, 1015 (1984).
- [89] M. V. Berry and M. Tabor, *Proc. R. Soc. A* **356**, 375 (1977).
- [90] Y. Y. Atas, E. Bogomolny, O. Giraud, and G. Roux, *Phys. Rev. Lett.* **110**, 084101 (2013).
- [91] D. N. Page, *Phys. Rev. Lett.* **71**, 1291 (1993).
- [92] G. De Tomasi and I. M. Khaymovich, *Phys. Rev. Lett.* **124**, 200602 (2020).
- [93] J. Chávez-Carlos, M. A. Bastarrachea-Magnani, S. Lerma-Hernández, and J. G. Hirsch, *Phys. Rev. E* **94**, 022209 (2016).
- [94] As evident from Fig. 3(b), the onset of chaos occurs at a faster rate for $\omega_0 \sim 1$ [as in Figs. 2(b)–2(d)], for which the π -oscillation remains unstable above QPT and is favorable for detection of chaos from spectral statistics.
- [95] M. V. Berry, *J. Phys. A* **10**, 2083 (1977).
- [96] R. Gati and M. K. Oberthaler, *J. Phys. B* **40**, R61 (2007); D. T. Pegg and S. M. Barnett, *Phys. Rev. A* **39**, 1665 (1989).
- [97] L. Pitaevskii and S. Stringari, *Phys. Rev. Lett.* **87**, 180402 (2001).
- [98] R. Gati, B. Hemmerling, J. Fölling, M. Albiez, and M. K. Oberthaler, *Phys. Rev. Lett.* **96**, 130404 (2006).
- [99] K. Baumann, C. Guerlin, F. Brennecke, and T. Esslinger, *Nature (London)* **464**, 1301 (2010); J. Klinder, H. Keßler, M. Wolke, L. Mathey, and A. Hemmerich, *Proc. Natl. Acad. Sci. U.S.A.* **112**, 3290 (2015).
- [100] M. P. Baden, K. J. Arnold, A. L. Grimsmo, S. Parkins, and M. D. Barrett, *Phys. Rev. Lett.* **113**, 020408 (2014).
- [101] I. Pietikäinen, J. Tuorila, D. S. Golubev, and G. S. Paraoanu, *Phys. Rev. A* **99**, 063828 (2019).
- [102] R. H. Dicke, *Phys. Rev.* **93**, 99 (1954).